ECCTD '93 – Circuit Theory and Design
H. Dedieu (Editor)

Signal-adaptive maximum likelihood filtering of ultrasonic speckle*

C. Kotropoulos X. Magnisalis I. Pitas M.G. Strintzis

Department of Electrical Engineering, University of Thessaloniki
Thessaloniki 540 06, Greece

1. INTRODUCTION

Speckle noise is a special kind of noise encountered in ultrasound (US) B-mode images as well as in images formed by laser beams or in synthetic aperture radar images. It is an interference effect caused by US beam scattering from microscopic tissue inhomogeneities [1]. Suppression of speckle is desirable in order to enhance the quality of US images and therefore increase the diagnostic potential of US examinations.

Motivated by the fact that signal-adaptive filters fulfill the requirements for successful speckle suppression and the attention they have attracted in the literature, signal-adaptive maximum likelihood (SAML) filters for ultrasonic speckle filtering are developed. Furthermore, a combined scheme where self-organizing neural networks such as the Learning Vector Quantizer [7] or its variant based on the L_2 mean [8] are used in conjunction with signal-adaptive filters is proposed in order to allow to allow image detail and edge preservation as well as maximum speckle reduction in homogeneous regions.

2. SIGNAL-ADAPTIVE MAXIMUM LIKELIHOOD FILTER DESIGN

An image x can be considered to consist of two parts: a low-frequency part x_L and a high-frequency part x_H, i.e., $x = x_L + x_H$ [4]. The low-frequency component is dominant in homogeneous image regions, whereas the high-frequency component is dominant near edges. The low-pass component can be estimated by a local estimator, e.g., the arithmetic mean or the median of the observations (i.e., pixel values) in a window $\mathcal{W}$ surrounding the current pixel (k,l) [4,5]. The maximum likelihood (ML) estimator $\hat{s}_{ML}(k,l)$ of the original signal $s(k,l)$ based on the observations $x(k-i,l-j) \in \mathcal{W}$ is proposed as the low-frequency component in this paper. Thus, the output of the signal-adaptive filter, i.e., the estimate of the original signal at (k,l), is given by:

$$\hat{s}(k,l) = \hat{s}_{ML}(k,l) + \beta(k,l)[x(k,l) - \hat{s}_{ML}(k,l)] \quad (1)$$

where $x(k,l)$ is the noisy observation at pixel (k,l), $\hat{s}_{ML}(k,l)$ is the maximum likelihood estimate of $s(k,l)$ based on the observations $x(k-i,l-j)$ and calculated over a window $\mathcal{W}$ surrounding pixel (k,l), and, $\beta(k,l)$ is a weighting factor, approximating the local SNR over the window $\mathcal{W}$.

Let us assume that ultrasonic speckle can be modeled as multiplicative Rayleigh distributed noise (in the case of envelope-detected US B-mode data), or as signal-dependent Gaussian noise (in the case of displayed US image data). The first model refers to envelope-detected US B-mode images [1,2]. In this case, the observed envelope-detected signal x is related to the original signal

* The research reported in this paper has been supported by ESPRIT Basic Research Action project NAT (7130). C. Kotropoulos has also been supported by a scholarship from the State Scholarship Foundation of Greece and the Bodosaki Foundation.

s by $x = sn$ where n is a noise term statistically independent of s. It has been proven that the ML estimator of a constant original signal $s = S$ based on N observations $X_1, X_2, \ldots, X_N$ assuming that n is a Rayleigh r.v. with unity expected value is given by [3]:

$$\hat{s}_{ML} = \frac{\sqrt{\pi}}{2}\sqrt{\frac{1}{N}\sum_{i=1}^{N} X_i^2} \tag{2}$$

which is equivalent to the L_2 mean [4] scaled by a factor of $\frac{\sqrt{\pi}}{2}$. The second model describes more accurately ultrasonic images where the displayed image data have undergone excessive manipulation (e.g. logarithmic compression, low and high-pass filtering, postprocessing, etc.) [2]. Therefore, let us assume the following image formation model: $x = s + s^{1/2}n$. It has also been proven that the ML estimate of S based on N observations $X_1, X_2, \ldots, X_N$ assuming that n is a zero-mean Gaussian random variable having variance σ^2 is given by [6]:

$$\hat{s}_{ML} = -\frac{\sigma^2}{2} + \sqrt{\frac{\sigma^4}{4} + \frac{1}{N}\sum_{i=1}^{N} X_i^2}. \tag{3}$$

Let $e(k,l) = \mathrm{E}_{\mathcal{W}}[(s - \hat{s})^2]$ denote the local mean squared error (MSE) between the noiseless signal $s(k,l)$ and its estimate $\hat{s}(k,l)$ obtained by (1) at pixel (k,l), where $\mathrm{E}_{\mathcal{W}}[\cdot]$ denotes a local expectation operator. It can easily shown that e can be rewritten as follows:

$$e = \mathrm{E}_{\mathcal{W}}[(s - \hat{s}_{ML})^2] + \beta^2 \mathrm{E}_{\mathcal{W}}[(x - \hat{s}_{ML})^2] - 2\beta \mathrm{E}_{\mathcal{W}}[(s - \hat{s}_{ML})(x - \hat{s}_{ML})]. \tag{4}$$

Differentiating with respect to β and setting the result equal to zero we get:

$$\beta = \begin{cases} 1 - \left(\frac{4-\pi}{4}\right)\frac{\mathrm{E}_{\mathcal{W}}[x^2]}{\mathrm{E}_{\mathcal{W}}[(x-\hat{s}_{ML})^2]} & \text{for the multiplicative noise model} \\ 1 - \frac{\mathrm{E}_{\mathcal{W}}[x]\sigma^2}{\mathrm{E}_{\mathcal{W}}[(x-\hat{s}_{ML})^2]} & \text{for the signal-dependent noise model.} \end{cases} \tag{5}$$

In general, β can be considered as a local signal-to-noise ratio measure [5]. The role of the signal-dependent weighting factor β (5) is to adjust the magnitude of the filtering to be performed by (1) as well as to adjust the size of window $\mathcal{W}$, i.e., to control how many pixels in the neighborhood of pixel (k,l) will be included in $\mathcal{W}$. We can start filtering by using initially a window of size 5×5 or 7×7. If the factor $\beta(k,l)$ becomes greater than an appropriate threshold β_t, the window size is decreased until the coefficient becomes less than the threshold or until the window reaches the size 3 ×3. Otherwise, the window is increased to its maximum size.

In the following, a modification of the SAML filter that utilizes segmentation information obtained prior to the filtering process is discussed. An image can be segmented into regions representing various image characteristics by a variety of techniques that can be found in digital image processing literature as well as by using self-organizing neural networks such as the LVQ [7] or its variant L_2 LVQ [8]. We shall focus on the neural network approach to ultrasonic image segmentation. Since the output neurons of L_2 LVQ correspond to the L_2 mean of input observations whereas those of LVQ correspond to the sample arithmetic mean of input observations, we conclude that L_2 LVQ is more suitable for ultrasonic images. Therefore, L_2 LVQ will be used to segment both simulated US images as well as real scans.

Let us denote by $\mathcal{L}(k,l)$ the class label assigned to pixel (k,l) of the original image by using an image segmentation algorithm. We shall assume that the original image is segmented into p classes. If the label assigned to the first class is 0, $\mathcal{L}(k,l)$ will vary between 0 and $p-1$. In

the case of a two-class US image segmentation, the label 0 can be assigned to pixels belonging to the background and the label 1 can be assigned to pixels that belong to areas that have high signal activity. In the general case of a p-class US image segmentation, label 0 is assigned to background pixels and the remaining classes are labeled according to their signal activity (e.g. frequency content). The classes that have the higher signal activity correspond to image details (e.g. boundaries of blood vessels). The more details an image region has the higher label is assigned to it. Let us also define by

$$\beta_{seg}(k,l) = \frac{1}{(p-1)\,N(\mathcal{W})} \sum_{(k-i,l-j)\in\mathcal{W}} \mathcal{L}(k-i,l-j) \tag{6}$$

a quantity that represents the average class label that appears in the filter window $\mathcal{W}$ scaled in the range $[0,1]$. In (6), $N(\mathcal{W})$ denotes the number of pixels included in the filter window (i.e., the window size). It can be seen that β_{seg} varies between 0 and 1. It tends to 0, when the pixels that belong in the lowest signal activity class dominate in the filter window $\mathcal{W}$ surrounding pixel (k,l). On the contrary, it tends to 1 when the pixels in the filter window $\mathcal{W}$ surrounding pixel (k,l) that belong to the highest signal activity class are in the majority. Since $\beta_{seg} \in [0,1]$, it can be used as weighting factor in the signal-adaptive filter (1). It is seen that by using (6) as weighting factor, the classes that correspond to image details are preserved. Furthermore, if the signal-adaptive filter has to share the benefits of the signal-dependent weighting factor (5) as local signal-to-noise ratio measure as well as of the factor (6) as local texture indicator, the following modified weighting factor $\hat{\beta}(k,l)$ is proposed:

$$\hat{\beta}(k,l) = (1-\eta)\beta(k,l) + \eta\beta_{seg}(k,l) \tag{7}$$

where $0 \leq \eta \leq 1$. By selecting $\eta = 0$, then $\hat{\beta}(k,l) = \beta(k,l)$ and the segmentation information provided by the image segmentation algorithm is discarded. If $\eta = 1$, $\hat{\beta}(k,l) = \beta_{seg}(k,l)$ and the local SNR information is ignored. Otherwise, both information sources are taken into account.

3. EXPERIMENTAL RESULTS

The performance of the modified signal-adaptive ML filter that utilizes segmentation information provided by the L_2 LVQ prior to filtering process is tested both on envelope-detected US B-mode images as well as on displayed images. Due to lack of space, only the results obtained for simulated envelope-detected US B-mode images will be described in this paper. Figure 1 shows an homogeneous tissue of size 4 cm $\times$ 4 cm with a lesion in the middle of diameter 2 cm. The amplitude of the reflections in the lesion is 5 dB stronger than the reflection strength in the background. Its resolution is 6 bits/pixel.

A Learning Vector Quantizer based on the L_2 mean has been created using 49 neurons at the first level corresponding to input patterns taken from a block of 7×7 pixels. The second level consists of 2 to 8 neurons corresponding to the output classes. A 7×7 window scans the image in a random manner to feed the network with input training patterns. During the recall phase, the 7×7 window scans the entire image in order to classify each pixel into one of p-many ($p = 2,\ldots,8$) classes. A parametric image is created containing the class membership of each pixel. In our case, two output classes have been used representing background and lesion respectively.

Next signal-adaptive filtering is combined with the ability of the L_2 LVQ to segment ultrasonic images in classes representing various tissue and lesion characteristics. The result of the overall filtering process using the modified signal-adaptive ML filter is presented in Figure 2.

Parameter η has been equal to 0.5 in (7). By comparing Figures 1 and 2, it can be seen that the proposed modification aids the filter in preserving better the edge information as well as acknowledging areas of the image containing valuable information that should not be filtered.

REFERENCES

1. J.G. Abbott and F.L. Thurstone, "Acoustic speckle: Theory and experimental analysis," *Ultrasonic Imaging*, vol. 1, pp. 303 324, 1979.

2. A. Loupas, "Digital image processing for noise reduction in medical ultrasonics," Ph.D dissertation, University of Edinburgh, U.K., July 1988.

3. C. Kotropoulos and I. Pitas, "Optimum nonlinear detection and estimation in the presence of ultrasonic speckle," *Ultrasonic Imaging*, vol. 14, pp. 249–275, 1992.

4. I. Pitas and A. N. Venetsanopoulos, *Nonlinear digital filters: Principles and Applications.* Dordrecht, The Netherlands: Kluwer Academic Publishers, 1990.

5. R. Bernstein, "Adaptive nonlinear filters for simultaneous removal of different kinds of noise in images," *IEEE Trans. on Circuits and Systems*, vol. CAS-34, no. 11, pp. 1275–1291, November 1987.

6. M.G. Strintzis, X. Magnisalis, C. Kotropoulos, I. Pitas and N. Maglaveras, "Maximum likelihood signal-adaptive filtering of speckle in ultrasound B-mode images," in *Proc. of the IEEE EMBS '92 Conf.*, Paris, France, November 1992.

7. T.K. Kohonen, "The self-organizing map," *Proceedings of the IEEE*, vol. 78, no. 9, pp. 1464–1480, September 1990.

8. C. Kotropoulos, X. Magnisalis, I. Pitas and M.G. Strintzis, "Nonlinear Ultrasonic Image Processing Based on Signal-Adaptive Filters and Self-Organizing Neural Networks," *IEEE Trans. on Image Processing*, accepted for publication.

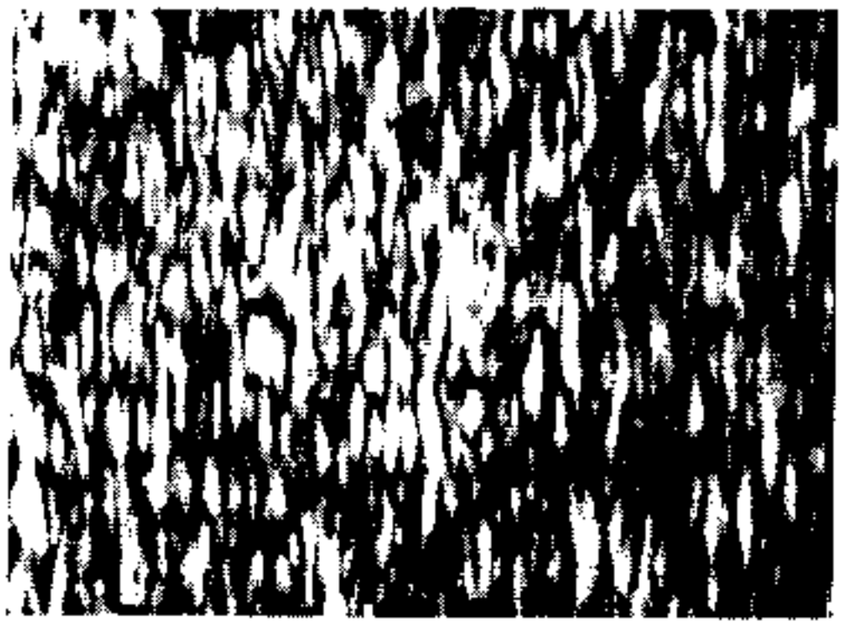

Figure 1. Simulation of an homogeneous piece of tissue with a circular lesion in the middle.

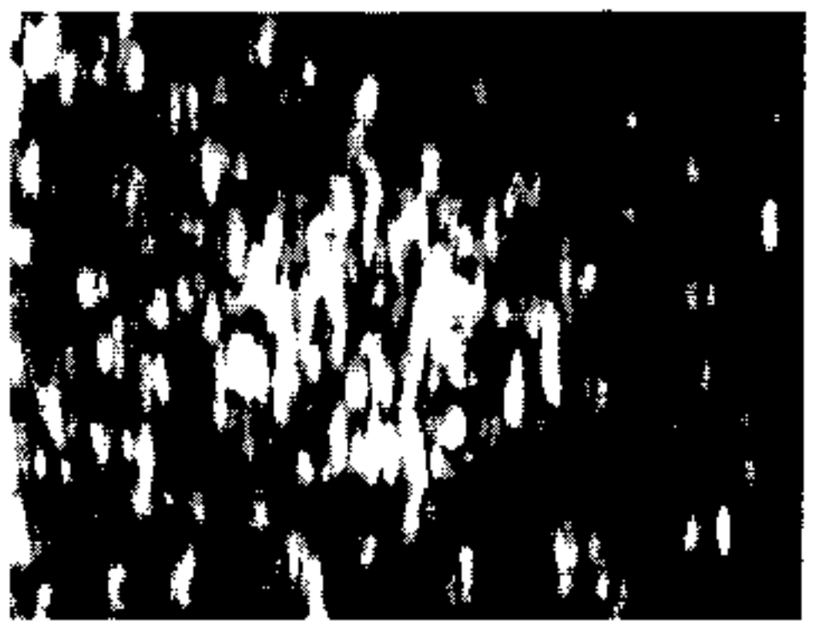

Figure 2. Results obtained by using segmentation in conjunction with filtering.